NEUROPATHOLOGY

Neuropathology 2010; **30**, 7–14 doi:10.1111/j.1440-1789.2009.01035.x

Original Article

Protein microarray analysis identifies cyclic nucleotide phosphodiesterase as an interactor of Nogo-A

Kenta Sumiyoshi,[1] Shinya Obayashi,[1] Hiroko Tabunoki,[1] Kunimasa Arima[2] and Jun-ichi Satoh[1]

[1]Department of Bioinformatics and Molecular Neuropathology, Meiji Pharmaceutical University, and [2]Department of Psychiatry, National Center Hospital, NCNP, Tokyo, Japan

Nogo-A, a neurite outgrowth inhibitor, is expressed exclusively on oligodendrocytes and neurons in the CNS. The central domain of Amino-Nogo spanning amino acids 567–748 in the human Nogo-A designated NIG, mediates persistent inhibition of axonal outgrowth and induces growth cone collapse by signaling through an as yet unidentified NIG receptor. We identified 82 NIG-interacting proteins by screening a high-density human protein microarray composed of 5000 proteins with a recombinant NIG protein as a probe. Following an intensive database search, we selected 12 neuron/oligodendrocyte-associated NIG interactors. Among them, we verified the molecular interaction of NIG with 2′, 3′-cyclic nucleotide 3′-phosphodiesterase (CNP), a cell type-specific marker of oligodendrocytes, by immunoprecipitation and cell imaging analysis. Although CNP located chiefly in the cytoplasm of oligodendrocytes might not serve as a cell-surface NIG receptor, it could act as a conformational stabilizer for the intrinsically unstructured large segment of Amino-Nogo.

Key words: CNP, NIG, Nogo-A, protein microarray, protein-protein interaction.

INTRODUCTION

Nogo is a family of myelin-associated inhibitors for axonal regeneration in the CNS.[1] It consists of three isoforms named A, B and C, all of which share a C-terminal 66 amino acid segment named Nogo-66. Nogo-A, the longest isoform with the strongest activity of neurite outgrowth inhibition, is expressed exclusively in myelin sheaths and oligodendrocytes on the cell surface and in the endoplasmic reticulum (ER), in addition to a subpopulation of neurons in the adult CNS. Nogo-A also plays a key role in maturation of oligodendrocytes *in vivo*.[2] Nogo-B is ubiquitously distributed both inside and outside the CNS, while Nogo-C, the shortest isoform, is enriched in skeletal muscle. Nogo-A has at least two discrete domains that exhibit neuronal growth-inhibitory activities.[3] One is located in the Nogo-A-specific C-terminal segment of Amino-Nogo, and the other is Nogo-66. The N-terminal segment of Amino-Nogo, shared between Nogo-A and Nogo-B, plays a role in vascular remodeling. Nogo-66, along with oligodendrocyte-myelin glycoprotein (OMgp) and myelin-associated glycoprotein (MAG), transduces inhibitory signals via a molecular complex composed of the Nogo receptor (NgR), Lingo-1, and $p75^{NTR}$ or Troy by activating RhoA that mediates actin depolymerization responsible for the collapse of growth cones on regenerating axons.[1]

The Nogo-A-specific C-terminal segment of Amino-Nogo, being conformationally unfolded,[4,5] mediates persistent inhibition of axonal outgrowth and induces growth cone collapse via the NgR-independent mechanism.[6] The central region of this segment spanning amino acids 567–748 in the human Nogo-A designated NIG, is pivotal for this activity.[3] Because the NIG domain exists only in Nogo-A, it provides an explanation for Nogo-A acting as the most potent inhibitor of axonal growth among three Nogo isoforms. Importantly, treatment with the antibody raised against the Nogo-A-specific domain enhances sprouting of corticospinal axons and promotes functional recovery following spinal cord injury in adult primates.[7] A previous study showed that the predominant proteins that

Correspondence: Jun-ichi Satoh, MD, Department of Bioinformatics and Molecular Neuropathology, Meiji Pharmaceutical University, 2-522-1 Noshio, Kiyose, Tokyo 204-8588, Japan. Email: satoj@my-pharm.ac.jp

Received 18 March 2009; Revised 13 April 2009; Accepted 14 April 2009; published online 7 June 2009.

interact with Nogo-A are Nogo-B and Nogo-C.[8] Although Amino-Nogo interacts with α5 and αv integrins,[9] the NIG-specific receptor remains to be characterized.

Recently, protein microarray technology has been established for rapid and systematic screening of protein-protein interactions in a high-throughput fashion.[10] The protein microarray is a chip on which thousands of functional proteins are immobilized. By reacting the array with the specific protein as a probe, it enables us to efficiently identify the target protein on chip as a binding partner. Protein microarray has a wide range of applications, including characterization of antibody specificity and autoantibody repertoire, and identification of novel biomarkers and molecular targets associated with disease type, stage and progression.[10] In the present study, we attempted to characterize a comprehensive profile of NIG-interacting proteins, which might include a candidate for NIG receptors, by using the high-density human protein microarray.

MATERIALS AND METHODS

Protein microarray analysis

We utilized ProtoArray v3.0 (Invitrogen, Carlsbad, CA, USA) that contains 5000 recombinant glutathione S-transferase (GST)-tagged human proteins expressed by the baculovirus expression system. They are purified to ensure the preservation of native structure, post-translational modifications, and proper functionality, as described previously.[11,12] The target proteins cover a wide range of biologically important proteins, and the complete list is shown in Table S1 online. The proteins are spotted on the glass slide in an arrangement of 4 × 12 subarrays equally spaced in vertical and horizontal directions. Because target proteins on the array protrude from the surface via N-terminal GST serving as a spacer, the probe is spatially accessible to all parts of them. Each subarray includes 20 × 20 spots, composed of 76 positive and negative control spots, 222 human target proteins, and 102 blanks and empty spots.

To prepare the probe for microarray analysis, the gene encoding the human NIG domain (NM_020532) was amplified by PCR with the primer set of 5′actggtacaaagat tgcttatgaa3′ and 5′aaataagtcaactggttcagaatc3′. It is worthy to note that the amino acid sequence of human NIG shows 82% and 80% identity to the rat or mouse ortholog, respectively. The PCR product was first cloned into the vector pSecTag/FRT/V5-His-TOPO (Invitrogen). Then, the gene segment coding for V5-tagged NIG was transferred into the vector pTrcHis-TOPO (Invitrogen). The V5-tagged NIG protein was expressed in *E. coli* and purified from the lysate by passing through the histidine-tagged proteins (HIS)-select spin column (Sigma, St. Louis, MO, USA), as described previously.[11,12] The purity and specificity of the probe were verified by silver stain and Western blot with mouse monoclonal anti-V5 antibody (Invitrogen) and sheep polyclonal anti-human NIG antibody (AF3515; R&D Systems, Minneapolis, MN, USA).

To block non-specific binding, the array was incubated at 4°C for 1 h with the phosphate-buffered saline supplemented with Tween 20 (PBST) blocking buffer, composed of 1% bovine serum albumin (BSA) and 0.1% Tween 20 in phosphate-buffered saline (PBS). Then, the array was incubated at 4°C for 90 min with the probe described above at a concentration of 100 μg/mL in the probing buffer, according to the methods described previously.[11,12] The array was then incubated at 4°C for 30 min with Alexa Fluor 647-conjugated mouse monoclonal anti-V5 antibody (Invitrogen). After washing, it was scanned by the GenePix 4200A scanner (Axon Instruments, Union City, CA, USA) at a wavelength of 635 nm. The data were analyzed by using the ProtoArray Prospector software v4.0 (Invitrogen), following acquisition of the microarray lot-specific information that compensates inter-lot variations among arrays in protein concentrations identified by the post-printing quality control. The spots showing the background-subtracted signal intensity value greater than the median plus three standard deviations of all the fluorescence intensities were considered as having significant interactions. The Z-score was calculated as the background-subtracted signal intensity value of the target protein minus the average of the background-subtracted signal intensity value from the negative control distribution, divided by the standard deviation of the negative control distribution. The cut-off value of Z-score was set as 3, as described previously.[11,12]

Immunoprecipitation and Western blot analysis

The coimmunoprecipitation analysis was performed according to the methods described previously.[11,12] In brief, the protein extract was prepared from the cells and tissues solubilized in mammalian protein extraction reagent (M-PER) protein extraction buffer (Pierce, Rockford, IL, USA). After preclearance, it was processed for immunoprecipitation with rabbit polyclonal anti-Nogo-A antibody (H-300; Santa Cruz Biotechnology, Santa Cruz, CA, USA) or rabbit polyclonal anti-2′, 3′-cyclic nucleotide 3′-phosphodiesterase (CNP) antibody (M-300; Santa Cruz Biotechnology). The precipitates were then processed for Western blot with anti-NIG antibody (AF3515) or mouse monoclonal anti-CNP antibody (11-5B; Sigma). The negative control included normal rabbit IgG instead of specific antibodies during the immunoprecipitation process. The specific reaction was visualized by using a chemiluminescence substrate (Pierce).

To specify the CNP-interacting domain of Nogo-A, the protein extract of HEK293 cells, in which the transgenes encoding NIG and CNP were coexpressed, was processed for coimmunoprecipition analysis. To achieve this, the NIG gene or the full-length CNP gene was amplified by PCR, and cloned into the expression vector p3XFLAG-CMV7.1 (Sigma) or pCMV-Myc (Clontech, Mountain View, CA, USA) to express a fusion protein with an N-terminal Flag or Myc tag, respectively. After cotransfection of the vectors in HEK293 cells, the protein extract was processed for immunoprecipitation with mouse monoclonal anti-Flag M2 affinity gel (Sigma) or rabbit polyclonal anti-Myc-conjugated agarose (Sigma). This was followed by Western blot with rabbit polyclonal anti-Myc antibody (Sigma) and mouse monoclonal anti-FLAG M2 antibody (Sigma).

Cell imaging, immunocytochemistry and immunohistochemistry

To determine coexpression of NIG and CNP in neural cell cultures, the NIG gene or the full-length CNP was cloned into the expression vector pDsRed-Express-C1 (Clontech) or pFN2A CMV Flexi (Promega, Madison, WI, USA) to express a fusion protein with an N-terminal DsRed or Halo tag, respectively. They were cotransfected in SK-N-SH neuroblastoma cells. At 24–48 h after transfection, the cells were exposed to Oregon Green (Promega), a fluorochrome specifically bound to the Halo tag protein. In some experiments, primary cultures established from the brain of newborn Institute of Cancer Research (ICR) mice were processed for double-immunolabeling with anti-NIG antibody (AF3515) and anti-CNP antibody (11-5B), followed by labeling with Alexa Fluor 568-conjugated anti-sheep IgG (Invitrogen) and Alexa Fluor 488-conjugated anti-mouse IgG (Invitrogen). Subsequently, the cells were fixed briefly in 4% paraformaldehyde, exposed to 4′, 6′-diamidino-2-phenylindole (DAPI; Invitrogen), mounted on slides with glycerol-polyvinyl alcohol, and examined on the Olympus BX51 universal microscope.

For double-labeling immunohistochemistry, deparaffinated tissue sections were heated in 10 mmol/L citrate sodium buffer, pH 6.0 by autoclave for 30 s at 125°C in a temperature-controlled pressure chamber (Dako, Tokyo, Japan). They were incubated with PBS containing 10% normal goat serum for 15 min at room temperature (RT) to block non-specific staining. Then, tissue sections were stained at RT overnight with anti-CNP antibody (11-5B), followed by incubation with alkaline phosphatase (AP)-conjugated anti-mouse IgG (Nichirei, Tokyo, Japan), and colorized with New Fuchsin substrate. After inactivation of the antibody by autoclaving the sections at 125°C for 30 s in 10 mM citrate sodium buffer, pH 6.0, the tissue sections were treated for 15 min with 3% hydrogen peroxide-containing distilled water to block the endogenous peroxidase activity. Then, they were relabeled with anti-Nogo-A antibody (H-300) or anti-NIG antibody (AF-3515), followed by incubation with horseradish peroxidase (HRP)-conjugated secondary antibodies, and colorized with DAB substrate and a counterstain with hematoxylin. For negative controls, the step of incubation with primary antibodies was omitted.

RESULTS

Protein microarray-identified 82 NIG interactors

For protein microarray analysis, we prepared a highly purified V5-tagged NIG probe showing a single 45-kDa band in a 12% SDS-PAGE gel (Fig. 1a, lanes 1–3). By screening the protein microarray with this probe, we identified 82 proteins as those showing significant interaction with NIG among 5000 proteins on the array. They are listed in Table S2 online. Because Nogo-A is located not only on the plasma membrane of oligodendrocytes, but also in the ER where the NIG domain is exposed to the cytosol,[13] it is not surprising that many extramembrane proteins are listed in NIG-interacting partners.

Selection of CNP as the most probable NIG interactor candidate

First, for 82 NIG interactors, we investigated the EST profile on UniGene (http://www.ncbi.nlm.nih.gov/UniGene), the protein expression profile on Human Protein Reference Database (HPRD; http://www.hprd.org), and the mRNA expression profile of mouse orthologs in the brain on the Allen Brain Atlas (ABA) database (http://www.brain-map.org), a high-throughput *in situ* hybridization atlas of gene expression pattern in the adult mouse brain.[14] The database search suggested that the great majority of 82 NIG interactors represent non-neural proteins, suggesting the promiscuous binding of most NIG interactors in a non-physiological setting on the array. Therefore, we focused exclusively on the proteins whose expression in the CNS is supported by the expression profiling on UniGene, HRPD and ABA databases. Subsequently, we identified the proteins highly relevant to the biological function of Nogo-A by searching on PubMed by importing brain, neuron, neurite, axon, myelin, or oligodendrocyte as search terms. Following intensive search, we retrieved 12 neuron/oligodendrocyte-associated NIG interactors that were hit by any of these key words (Table 1). Among them, we finally found that only CNP (the spots in Fig. 1b), a cell type-specific marker for oligodendrocytes, has a physiological relevance to axon, myelin and oligodendrocytes (see the details in the Discussion section).

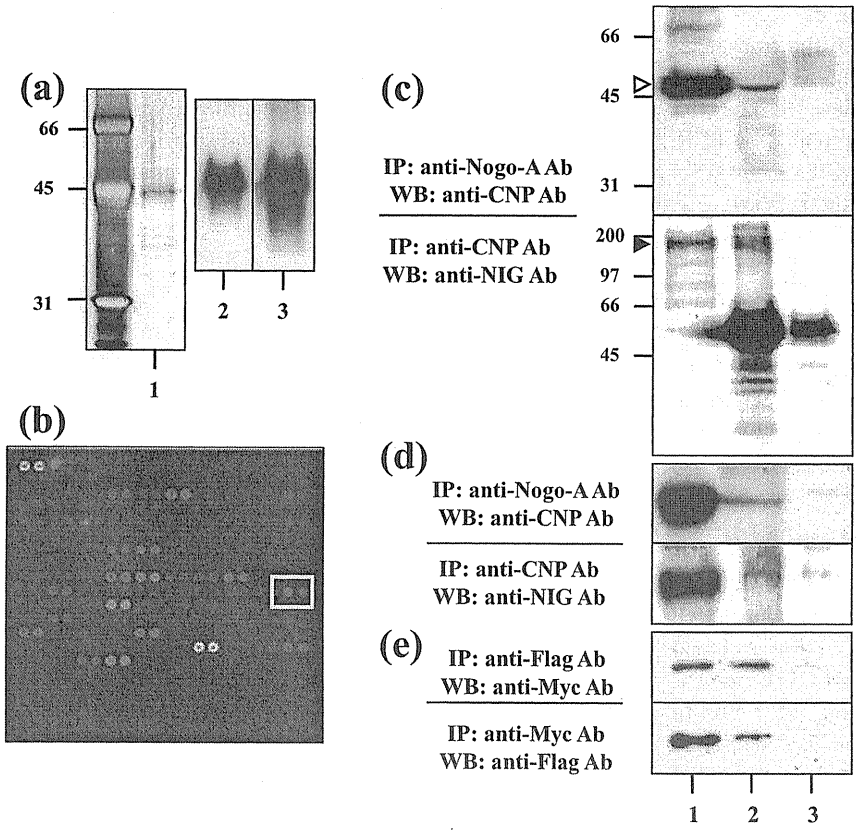

Fig. 1 Protein microarray and immunoprecipitation analysis. (a) The V5-tagged NIG-specific probe utilized for microarray analysis. The probe (0.3 μg each lane) was separated by a 12% SDS-PAGE gel. The silver stain of the gel with the position of molecular weight markers (lane 1). The blot was labeled with anti-V5 antibody (lane 2) and anti-human NIG antibody (lane 3). (b) Anti-2′, 3′-cyclic nucleotide 3′-phosphodiesterase (CNP) identified as a NIG interactor on the array. The protein microarray containing duplicate spots of 5000 proteins is composed of 4 × 12 subarrays. Each subarray includes 20 × 20 spots, composed of 76 control spots, including 14 positive and 62 negative control spots, 222 human target proteins, and 102 blanks and empty spots. The subarray No. 20 is shown. The spots positioned at row 10, columns 19, 20 indicated by an enclosed yellow line represent CNP. (c–e) Immunoprecipitation (IP) and Western blot (WB). Anti-Nogo-A antibody pulled down the endogenous CNP (open arrow, 47-kDa), while anti-CNP antibody precipitated the endogenous full-length Nogo-A (filled arrow, 190-kDa) from (c) the human brain homogenate, and from (d) the rat C6 glioma cell lysate. (e) The NIG gene and the CNP gene were cloned into the expression vectors to express a fusion protein with a Flag or Myc tag, respectively. They were cotransfected in HEK293 cells, and the lysate was processed for immunoprecipitation analysis with anti-Flag antibody and anti-Myc antibody. The lanes (1–3) of (c–e) represent (1) input control, (2) IP with the target-specific antibody, and (c) IP with normal mouse or rabbit IgG.

Validation of the interaction between NIG and CNP

Next, we verified the molecular interaction between Nogo-A and CNP by coimmunoprecipitation analysis. Anti-Nogo-A antibody (H-300) pulled down the endogenous CNP (47-kDa) labeled with anti-CNP antibody, while anti-CNP antibody (M-300) precipitated the full-length Nogo-A (190-kDa) labeled with anti-NIG antibody from both the human brain homogenate and the lysate of rat C6 glioma cells (Fig. 1c,d, upper and lower panels, lane 2). In contrast, the inclusion of normal IgG instead of H-300 or M-300 antibody recovered neither CNP nor Nogo-A (Fig. 1c,d, upper and lower panels, lane 3), supporting the specificity of the interaction. These results indicate that the endogenous Nogo-A interacts with the endogenous CNP *in vitro* and *in vivo*.

To specify the CNP-interacting domain of Nogo-A, the NIG gene or the CNP gene was cloned into the two different expression vectors to express a fusion protein with an N-terminal Flag or Myc tag. After cotransfection of the vectors in HEK293 cells, the protein extract was processed for immunoprecipitation with mouse monoclonal anti-Flag M2 affinity gel, rabbit polyclonal anti-Myc-conjugated agarose, or the same amount of normal mouse or rabbit IgG-conjugated agarose, followed by Western blot with rabbit polyclonal anti-Myc antibody and mouse monoclonal anti-FLAG M2 antibody. The reciprocal coimmunoprecipitation analysis verified the interaction of the NIG domain of Nogo-A and CNP (Fig. 1e, upper and lower panels, lane 2). These results indicate that the NIG domain of Nogo-A on its own interacts with CNP, but do not exclude the possibility that the domain located outside NIG is also bound to CNP.

To determine subcellular colocation of NIG and CNP, the NIG gene or the CNP gene was cloned into the two different expression vectors to express a fusion protein with an N-terminal DsRed or Halo tag. When cotransfected in SK-N-SH neuroblastoma cells, NIG was expressed not only on the plasma membrane but also in the cytoplasm, and at low amounts in the nucleus. DsRed-tagged NIG and Oregon Green-labeled CNP were coexpressed chiefly in the cytoplasm (Fig. 2, panels a–c). Furthermore, coexpression of NIG and CNP was identified

Table 1 Twelve neuron/oligodendrocyte-associated NIG interactors

No.	Gene symbol	Gene name	Z-score	Putative function
1	RPL31	Ribosomal protein L31	7.22386	A ribosomal protein that constitutes a component of the 60S subunit
2	CIRBP	Cold inducible RNA binding protein	6.76639	A cold-shock protein that plays a role in cold-induced suppression of cell proliferation
3	PLK3	Polo-like kinase 3 (Drosophila)	6.51572	A serine/threonine kinase that plays a role in regulation of cell cycle progression
4	MARK4	MAP/microtubule affinity-regulating kinase 4	5.45038	A serine/threonine kinase involved in microtubule organization in neuronal cells
5	RPL30	Ribosomal protein L30	4.82371	A ribosomal protein that constitutes a component of the 60S subunit
6	CNP	2′,3′-cyclic nucleotide 3′ phosphodiesterase	4.71717	A membrane-bound enzyme located in the CNS myelin
7	FGF13	Fibroblast growth factor 13	4.35684	A member of the fibroblast growth factor family
8	ZNF192	Zinc finger protein 192	4.09363	A transcription factor of unknown function
9	NHP2	Nucleolar protein family A, member 2 (H/ACA small nucleolar RNPs)	4.04663	A member of the H/ACA snoRNPs gene family
10	ATP5O	ATP synthase, H+ transporting, mitochondrial F1 complex, O subunit (oligomycin sensitivity conferring protein)	3.25389	A component of the F-type ATPase located in the mitochondrial matrix
11	ODC1	Ornithine decarboxylase 1	3.06902	The rate-limiting enzyme of the polyamine biosynthesis pathway that catalyzes ornithine to putrescine
12	EIF2C1	Eukaryotic translation initiation factor 2C, 1	3.00322	A member of the Argonaute family that plays a role in RNA interference

Among 82 NIG interactor candidates (Table S2), 12 were categorized as neuron/oligodendrocyte-associated NIG interactors by database search on UniGene, HPRD, and Allen Brain Atlas, and by the PubMed search with brain, neuron, neurite, axon, myelin, or oligodendrocyte as search terms. Among them, we found that only CNP (No. 6) has a physiological relevance to axon, myelin and oligodendrocytes.

both in the cytoplasm and on the cell surface of highly-branched differentiated oligodendrocytes consisting of a small population of newborn mouse brain cell cultures (Fig. 2, panels d–f).

Finally, we studied coexpression of Nogo-A and CNP *in vivo* in the human brain by immunohistochemistry. A substantial overlap was found in the expression pattern of Nogo-A, NIG and CNP in oligodendrocytes and myelin sheaths of the cerebral white matter (Fig. 2, panels g and h), supporting the possibility that Nogo-A *in vivo* interacts with CNP, probably by binding via the NIG domain.

DISCUSSION

Protein microarray serves as a powerful tool for the rapid and systematic identification of protein-protein and other biomolecule interactions.[10] Protein microarray has a wide range of applications, including characterization of antibody specificity and autoantibody repertoire, and identification of novel biomarkers and molecular targets associated with disease type, stage and progression, leading to establishment of personalized medicine.[10] When a specific probe is available, the whole experimental procedure of protein microarray analysis requires the exact time shorter than 5 h to obtain the complete list of interacting proteins on the array.[11,12]

However, protein microarray technology is still under development in methodological aspects.[10–12] In general, protein microarray has its own limitations associated with the expression and purification of a wide variety of target proteins. In the microarray we utilized, the target proteins were expressed in a baculovirus expression system, purified under native conditions, and spotted on the slides to ensure the preservation of native structure, post-translational modifications such as glycosylation and phophorylation, and proper functionality. In contrast, bacterially expressed proteins lack glycosylation and phosphorylation moieties, and are often misfolded during purification. Since target proteins contain a GST fusion tag, the arrays are always processed for the post-spotting quality control by using an anti-GST antibody with a concentration gradient of GST spots as a standard. This procedure makes it possible to quantify the exact amount of proteins deposited in each spot, and thereby minimizes the inter-lot variability of the results. Furthermore, each subarray contains a series of built-in control spots.

Protein microarray also has another technical limitation attributable to the avidity of protein-protein interaction.[10–12] The probing and rigorous washing procedure detects mostly the direct protein-protein interaction supported by the stable binding ability. It could not efficiently detect much weak and transient protein-protein interactions, or indirect interactions that require accessory molecules or intervening cofactors. In addition,

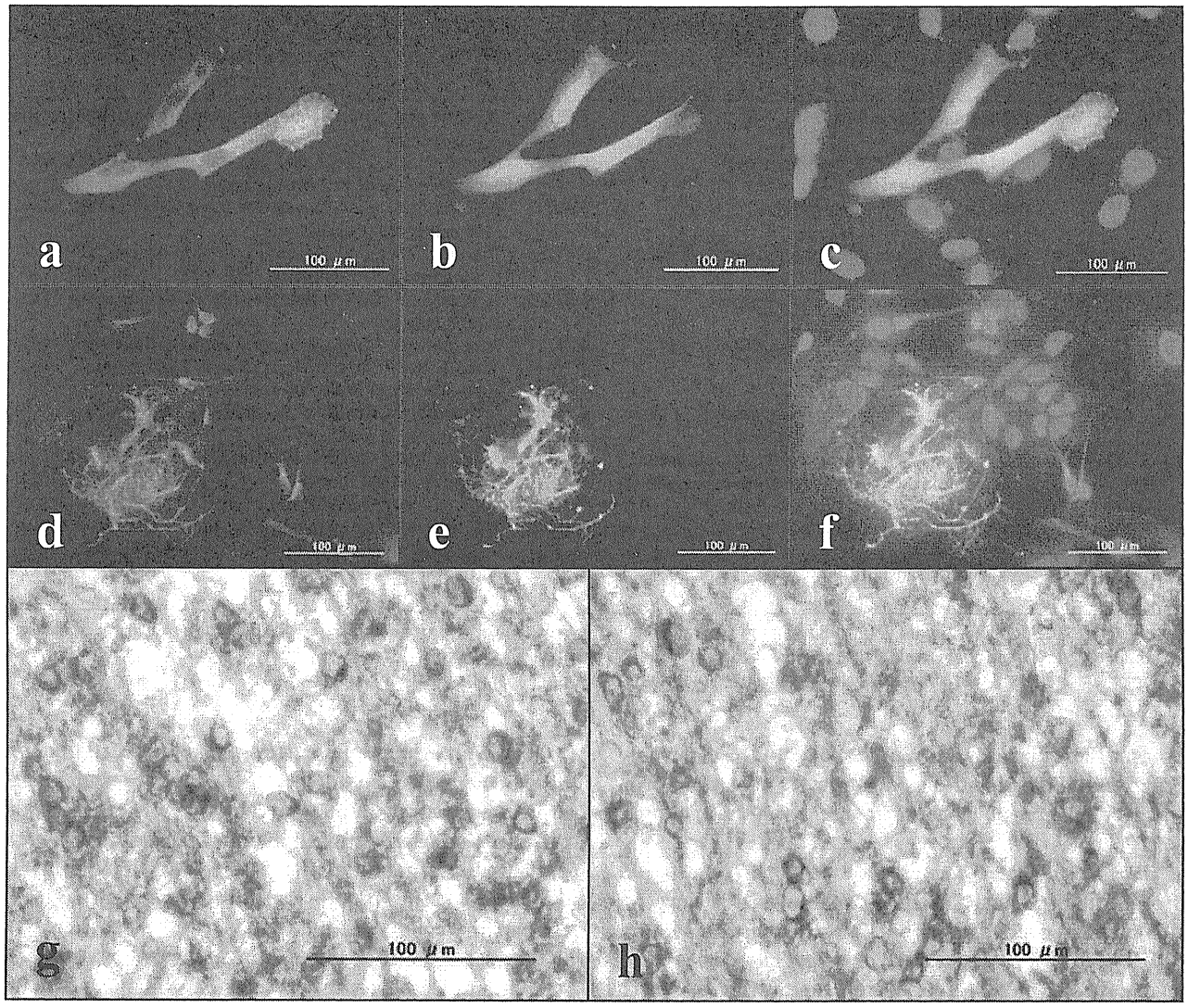

Fig. 2 Coexpression of NIG and anti-2′, 3′-cyclic nucleotide 3′-phosphodiesterase (CNP). (a–c) SK-N-SH neuroblastoma cells. The NIG gene and the CNP gene were cloned into the expression vectors to express a fusion protein with a DsRed or Halo tag, and they were cotransfected in SK-N-SH cells. (a) DsRed-labeled NIG, (b) Oregon Green-labeled CNP, and (c) merge (a) and (b) with 4′, 6′-diamidino-2-phenylindole (DAPI). (d–f) Newborn mouse brain cell cultures. Primary cultures established from newborn ICR mice double immunolabeled with anti-NIG antibody (AF3515) and anti-CNP antibody (11-5B), followed by labeling with Alexa Fluor 568-conjugated anti-sheep IgG and Alexa Fluor 488-conjugated anti-mouse IgG. (d) NIG, (e) CNP, and (f) merge (d) and (e) with DAPI. (g,h) Human brain tissues. The human brain tissue section derived from the peri-infarct white matter of the frontal cortex of a 62-year-old male with middle cerebral artery occlusion was double immunolabeled with (g) anti-Nogo-A antibody (H-300; brown) and anti-CNP antibody (11-5B; red) and (h) anti-NIG antibody (AF3515; brown) and anti-CNP antibody (11-5B; red).

protein microarray screening does not consider the specific subcellular location where the protein-protein interaction actually takes place. Thus, it is possible that some promiscuous partners are detected, whereas some biologically important interactors *in vivo* are left beyond identification. Therefore, protein microarray data always require the validation by other independent methods such as coimmunoprecipitation, Western blotting, the yeast two-hybrid (Y2H) screening, and so on. Post-translational modifications play a pivotal role in a range of protein-protein interactions. Immunolabeling of the array we utilized with anti-phosphotyrosine antibody showed that approximately 10–20% of the proteins on the array are phosphorylated (unpublished data of Invitrogen). When the array was applied for kinase substrate identification, most known kinases immobilized on the array are enzymatically active with the capacity of autophosphorylation, suggesting that they are functionally

active with preservation of proper conformation (unpublished data of Invitrogen).

Previous studies indicate that the central domain of Amino-Nogo spanning amino acids 567–748 in the human Nogo-A designated NIG mediates persistent inhibition of axonal outgrowth and induces growth cone collapse by signaling through an as yet unidentified NIG receptor.[3] To characterize NIG-interacting proteins that might include an NIG receptor, we screened the high-density human protein microarray composed of 5000 proteins with a recombinant NIG protein as a probe. However, most of the 82 NIG interactors identified by protein microarray analysis are non-neural proteins, suggesting promiscuous binding in a non-physiological setting on the array. Therefore, we focused exclusively on the proteins whose expression in the CNS is supported by the expression profiling on UniGene, HRPD and ABA databases. Subsequently, we searched them on PubMed and retrieved 12 neuron/oligodendrocyte-associated NIG interactors (Table 1). Among them, we finally identified CNP as the most probable candidate in view of a physiological relevance to axon, myelin and oligodendrocytes. CNP is a valid cell type-specific marker for oligodendrocytes, essential for axonal support but not for myelin assembly.[15] CNP acts as a membrane anchor for tubulin required for process outgrowth of oligodendrocytes,[16,17] and ubiquitinated CNP is concentrated within lipid rafts,[18] suggesting that CNP expressed intracellularly in the cytoplasm is located in close proximity to the cell membrane where Nogo-A is accumulated. Therefore, we considered CNP as the most feasible NIG interactor candidate *in vivo*. The interaction of NIG with CNP and their coexpression in both oligodendrocytes and myelin were validated by immunoprecipitation, cell imaging, and immunolabeling.

Previously, we and others showed that Nogo-A expression is greatly enhanced in surviving oligodendrocytes and CNP is expressed in damaged but still remaining myelin sheaths, while NgR is upregulated in reactive astrocytes and macrophages/microglia at the edge of chronic active demyelinating lesions of multiple sclerosis (MS),[19,20] suggesting a pathological role of Nogo-A/NgR interaction in persistent demyelination and loss of axonal regeneration in MS lesions. Interestingly, a certain population of MS patients shows enhanced T-cell and B-cell responses against CNP and Nogo-A, suggesting that both CNP and Nogo-A serve as autoantigens.[21,22] Nogo-A takes at least two different membrane topologies in oligodendrocytes,[3,8] where it is possible that the N-terminal region of Nogo-A is exposed to the extracellular space or is located in the cytoplasm. Because CNP is expressed primarily in the cytoplasm of oligodendrocytes, it might not serve as a cell-surface NIG receptor possibly expressed on axons and neurons that transduces the signals for inhibition of axonal outgrowth and induction of growth cone collapse. However, the possibility exists that CNP could act as an intracellular conformational stabilizer for the intrinsically-unstructured unstable Amino-Nogo segment in oligodendrocytes (Fig. 3).

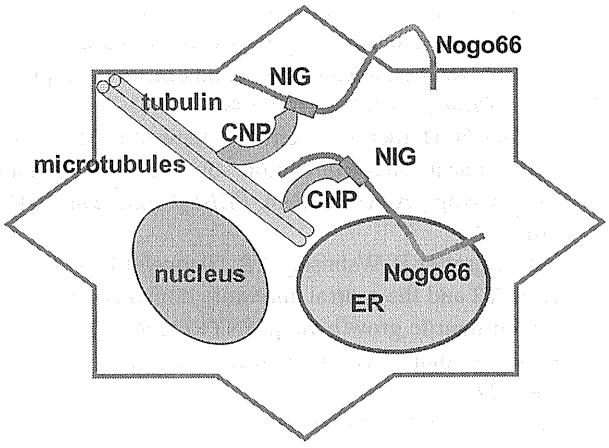

Fig. 3 A hypothetical model of NIG and anti-2′, 3′-cyclic nucleotide 3′-phosphodiesterase (CNP) interaction in oligodendrocytes. CNP (the orange piece) acts as a membrane anchor for tubulin essential for process outgrowth of oligodendrocytes, located in close proximity to the plasma membrane and possibly to the ER membrane where Nogo-A is accumulated. By interacting with NIG (the grey box), CNP serves as an intracellular conformational stabilizer for the intrinsically unstructured large segment of Amino-Nogo.

ACKNOWLEDGMENTS

All autopsied brain samples obtained under written informed consent were provided by Research Resource Network (RRN), Japan. This work was supported by a research grant to J-IS from the High-Tech Research Center Project, the Ministry of Education, Culture, Sports, Science and Technology (MEXT), Japan (S0801043).

REFERENCES

1. Walmsley AR, Mir AK. Targeting the Nogo-a signalling pathway to promote recovery following acute CNS injury. *Curr Pharm Des* 2007; **13**: 2470–2484.
2. Pernet V, Joly S, Christ F, Dimou L, Schwab ME. Nogo-A and myelin-associated glycoprotein differently regulate oligodendrocyte maturation and myelin formation. *J Neurosci* 2008; **28**: 7435–7444.
3. Oertle T, van der Haar ME, Bandtlow CE *et al.* Nogo-A inhibits neurite outgrowth and cell spreading with three discrete regions. *J Neurosci* 2003; **23**: 5393–5406.

4. Li M, Song J. The N- and C-termini of the human Nogo molecules are intrinsically unstructured: bioinformatics, CD, NMR characterization, and functional implications. *Proteins* 2007; **68**: 100–108.
5. Zander H, Hettich E, Greiff K, Chatwell L, Skerra A. Biochemical characterization of the recombinant human Nogo-A ectodomain. *FEBS J* 2007; **274**: 2603–2613.
6. Schweigreiter R, Walmsley AR, Niederöst B *et al.* Versican V2 and the central inhibitory domain of Nogo-A inhibit neurite growth via p75NTR/NgR-independent pathways that converge at RhoA. *Mol Cell Neurosci* 2004; **27**: 163–174.
7. Freund P, Schmidlin E, Wannier T *et al.* Nogo-A-specific antibody treatment enhances sprouting and functional recovery after cervical lesion in adult primates. *Nat Med* 2006; **12**: 790–792.
8. Dodd DA, Niederoest B, Bloechlinger S, Dupuis L, Loeffler JP, Schwab ME. Nogo-A, -B, and -C are found on the cell surface and interact together in many different cell types. *J Biol Chem* 2005; **280**: 12494–12502.
9. Hu F, Strittmatter SM. The N-terminal domain of Nogo-A inhibits cell adhesion and axonal outgrowth by an integrin-specific mechanism. *J Neurosci* 2008; **28**: 1262–1269.
10. Schweitzer B, Predki P, Snyder M. Microarrays to characterize protein interactions on a whole-proteome scale. *Proteomics* 2003; **3**: 2190–2199.
11. Satoh J, Nanri Y, Yamamura T. Rapid identification of 14-3-3-binding proteins by protein microarray analysis. *J Neurosci Methods* 2006; **152**: 278–288.
12. Satoh J, Obayashi S, Misawa T, Sumiyoshi K, Oosumi K, Tabunoki H. Protein microarray analysis identifies human cellular prion protein interactors. *Neuropathol Appl Neurobiol* 2009; **35**: 16–35.
13. Voeltz GK, Prinz WA, Shibata Y, Rist JM, Rapoport TA. A class of membrane proteins shaping the tubular endoplasmic reticulum. *Cell* 2006; **124**: 573–586.
14. Lein ES, Hawrylycz MJ, Ao N *et al.* Genome-wide atlas of gene expression in the adult mouse brain. *Nature* 2007; **445**: 168–176.
15. Lappe-Siefke C, Goebbels S, Gravel M *et al.* Disruption of Cnp1 uncouples oligodendroglial functions in axonal support and myelination. *Nat Genet* 2003; **33**: 366–374.
16. Bifulco M, Laezza C, Stingo S, Wolff J. 2′,3′-Cyclic nucleotide 3′-phosphodiesterase: a membrane-bound, microtubule-associated protein and membrane anchor for tubulin. *Proc Natl Acad Sci USA* 2002; **99**: 1807–1812.
17. Lee J, Gravel M, Zhang R, Thibault P, Braun PE. Process outgrowth in oligodendrocytes is mediated by CNP, a novel microtubule assembly myelin protein. *J Cell Biol* 2005; **170**: 661–673.
18. Hinman JD, Chen CD, Oh SY, Hollander W, Abraham CR. Age-dependent accumulation of ubiquitinated 2′, 3′-cyclic nucleotide 3′-phosphodiesterase in myelin lipid rafts. *Glia* 2008; **56**: 118–133.
19. Satoh J, Onoue H, Arima K, Yamamura T. Nogo-A and nogo receptor expression in demyelinating lesions of multiple sclerosis. *J Neuropathol Exp Neurol* 2005; **64**: 129–138.
20. Kuhlmann T, Remington L, Maruschak B, Owens T, Brück W. Nogo-A is a reliable oligodendroglial marker in adult human and mouse CNS and in demyelinated lesions. *J Neuropathol Exp Neurol* 2007; **66**: 238–246.
21. Muraro PA, Kalbus M, Afshar G, McFarland HF, Martin R. T cell response to 2′,3′-cyclic nucleotide 3′-phosphodiesterase (CNPase) in multiple sclerosis patients. *J Neuroimmunol* 2002; **130**: 233–242.
22. Onoue H, Satoh JI, Ogawa M, Tabunoki H, Yamamura T. Detection of anti-Nogo receptor autoantibody in the serum of multiple sclerosis and controls. *Acta Neurol Scand* 2007; **115**: 153–160.

SUPPORTING INFORMATION

Additional Supporting Information may be found in the online version of this article:

Table S1 The complete list of the proteins immobilized on a human protein microarray utilized in the present study
Table S2 The list of 82 NIG interactors identified by protein microarray

Please note: Wiley-Blackwell are not responsible for the content or functionality of any supporting materials supplied by the authors. Any queries (other than missing material) should be directed to the corresponding author for the article.

Cell Mol Neurobiol (2010) 30:415–426
DOI 10.1007/s10571-009-9466-3

ORIGINAL RESEARCH

Stable Expression of Neurogenin 1 Induces LGR5, a Novel Stem Cell Marker, in an Immortalized Human Neural Stem Cell Line HB1.F3

Jun-ichi Satoh · Shinya Obayashi · Hiroko Tabunoki · Taeko Wakana · Seung U. Kim

Received: 15 August 2009 / Accepted: 25 September 2009 / Published online: 8 October 2009

Abstract Neural stem cells (NSC) with self-renewal and multipotent properties serve as an ideal cell source for transplantation to treat spinal cord injury, stroke, and neurodegenerative diseases. To efficiently induce neuronal lineage cells from NSC for neuron replacement therapy, we should clarify the intrinsic genetic programs involved in a time- and place-specific regulation of human NSC differentiation. Recently, we established an immortalized human NSC clone HB1.F3 to provide an unlimited NSC source applicable to genetic manipulation for cell-based therapy. To investigate a role of neurogenin 1 (Ngn1), a proneural basic helix-loop-helix (bHLH) transcription factor, in human NSC differentiation, we established a clone derived from F3 stably overexpressing Ngn1. Genome-wide gene expression profiling identified 250 upregulated genes and 338 downregulated genes in Ngn1-overexpressing F3 cells (F3-Ngn1) versus wild-type F3 cells (F3-WT). Notably, leucine-rich repeat-containing G protein-coupled receptor 5 (LGR5), a novel stem cell marker, showed an 167-fold increase in F3-Ngn1, although transient overexpression of Ngn1 did not induce upregulation of LGR5, suggesting that LGR5 is not a direct transcriptional target of Ngn1. KeyMolnet, a bioinformatics tool for analyzing molecular relations on a comprehensive knowledgebase, suggests that the molecular network of differentially expressed genes involves the complex interaction of networks regulated by multiple transcription factors. Gene ontology (GO) terms of development and morphogenesis are enriched in upregulated genes, while those of extracellular matrix and adhesion are enriched in downregulated genes. These results suggest that stable expression of a single gene Ngn1 in F3 cells induces not simply neurogenic but multifunctional changes that potentially affect the differentiation of human NSC via a reorganization of complex gene regulatory networks.

Keywords HB1.F3 · KeyMolnet · LGR5 · Microarray · Neural stem cells · Neurogenin 1

Electronic supplementary material The online version of this article (doi:10.1007/s10571-009-9466-3) contains supplementary material, which is available to authorized users.

J. Satoh (✉) · S. Obayashi · H. Tabunoki · T. Wakana
Department of Bioinformatics and Molecular Neuropathology, Meiji Pharmaceutical University, 2-522-1 Noshio, Kiyose, Tokyo 204-8588, Japan
e-mail: satoj@my-pharm.ac.jp

S. U. Kim
Division of Neurology, Department of Medicine, University of British Columbia Hospital, University of British Columbia, Vancouver, BC, Canada

S. U. Kim
Medical Research Institute, Chung-Ang University College of Medicine, Seoul, Korea

Abbreviations

bHLH	Basic helix-loop-helix
CNS	Central nervous system
DAVID	Database for annotation visualization and integrated discovery
DEG	Differentially expressed genes
FBS	Fetal bovine serum
GAS2	Growth arrest-specific 2
GO	Gene ontology
HAS2	Hyaluronan synthase 2
LGR5	Leucine-rich repeat-containing G protein-coupled receptor 5
MMP9	Matrix metallopeptidase 9
Ngn1	Neurogenin 1

NPC	Neural progenitor cells
NSC	Neural stem cells
ORF	Open-reading frame
RMA	Robust multiarray average
RT-PCR	Reverse transcription-polymerase chain reaction
SHH	Sonic hedgehog homolog
Wnt	Wingless-type MMTV integration site family

Introduction

Neural stem cells (NSC) with self-renewal and multipotent properties serve as an ideal cell source for transplantation to treat spinal cord injury, stroke, and neurodegenerative diseases (Kim 2004; Kim and de Vellis 2009). To efficiently induce neuronal lineage cells from NSC for neuron replacement therapy, we should clarify the intrinsic genetic programs involved in a time- and place-specific regulation of human NSC differentiation. Previously, we found that primary cultures of human neural progenitor cells (NPC) exhibit an intrinsic capacity to differentiate into astrocytes in response to bone morphogenic protein 4 (BMP4) included in the serum (Obayashi et al. 2009). This might be a major hindrance against the proper commitment to neuronal linage cells following transplantation of NSC in vivo. Recently, we established an immortalized human NSC clone HB1.F3 by retroviral vector-mediated v-myc gene transfer into fetal human telencephalon cell cultures (Kim 2004). HB1.F3 cells could provide an unlimited NSC source applicable to genetic manipulation ex vivo for cell-based therapy. Actually, F3 cells stably expressing therapeutic genes migrate and integrate into target brain tissues upon transplantation in animal models of Parkinson disease, Huntington disease, and amyotrophic lateral sclerosis, and they differentiate into neurons, followed by an enhanced functional recovery (Kim et al. 2006; Kim and de Vellis 2009).

Neurogenin-1 (NEUROG1, Ngn1) is a member of proneural basic helix-loop-helix (bHLH) transcription factors that promote neurogenesis by activating a battery of target genes, including the NeuroD family of bHLH transcription factors (Morrison 2001). During embryogenesis, Ngn1 is expressed in NPC distributed in dorsal root ganglia (DRG), dorsal and ventral regions of the neural tube, dorsal telencephalon, and specific regions within the midbrain and hindbrain (Sommer et al. 1996). Although there exists a functional redundancy among Ngn1, Ngn2, and Ngn3, Ngn1-deficient mice failed to generate a $TrkA^+$ subset of cervical DRG neurons (Ma et al. 1999). Overexpression of Ngn1 induces neurite outgrowth in F11 rat DRG and mouse neuroblastoma hybrid cells (Kim et al. 2002). Stable expression of Ngn1 induces neuronal differentiation of pluripotent mouse embryonal carcinoma P19 cells (Kim et al. 2004). Ngn1 inhibits differentiation of rat NSC into astrocytes by sequestering a transcriptional coactivator complex composed of CBP and SMAD1 and blocking activation of STAT transcription factors (Sun et al. 2001).

In the present study, to investigate the role of Ngn1 in human NSC differentiation, we established a clonal cell line stably overexpressing Ngn1 by retroviral vector-mediated gene transfer into HB1.F3 cells. Then, we studied genome-wide gene expression profiles of Ngn1-overexpressing F3 cells (F3-Ngn1) and wild-type F3 cells (F3-WT) by using whole genome DNA microarrays. As a result, we unexpectedly found that stable expression of a single gene Ngn1 in F3 cells induced a robust upregulation of leucine-rich repeat-containing G protein-coupled receptor 5 (LGR5), a recently identified marker for intestine and hair follicle stem cells (Barker et al. 2007; Jaks et al. 2008; Sato et al. 2009). Our results suggested that stable expression of Ngn1 in human NSC cells induces not only simply neurogenic but also multifunctional changes that potentially affect the differentiation of NSC via a reorganization of complex gene regulatory networks.

Methods

Human Neural Stem Cell Clone HB1.F3 and Its Derivative HB1.F3-Ngn1

Primary cultures of fetal human telencephalon cells were transformed with a retroviral vector pLSNmyc carrying the v-myc oncogene and the neomycin resistance gene. Following selection with G418, a single continuously dividing clone with a capacity to self-renew and differentiate into neurons and glial cells both in vitro and in vivo was isolated and designated HB1.F3 (Kim 2004). It carried normal human karyotype of 46 XX. After transducing a retroviral vector pBabePNgn1 carrying the open-reading frame (ORF) of the human Ngn1 gene and the puromycin resistance gene into HB1.F3 cells, a single puromycin-resistant clone was selected, expanded, and designated HB1.F3-Ngn1. In the present study, the wild-type HB1.F3 cells and the HB1.F3-Ngn1 cells are abbreviated as F3-WT and F3-Ngn1. They were incubated in the feeding medium composed of Dulbecco's modified Eagle's medium (DMEM) (Invitrogen, Carlsbad, CA, USA) supplemented with 10% fetal bovine serum (FBS), 100 U/ml penicillin and 100 μg/ml streptomycin. The medium was renewed every 3 days.

Microarray Analysis

Total RNA was isolated from subconfluent cells by using the TRIZOL Plus RNA Purification kit (Invitrogen). The

quality of total RNA was evaluated on Agilent 2100 Bioanalyzer (Agilent Technologies, Palo Alto, CA, USA). One hundred nanograms of total RNA was processed for cRNA synthesis, fragmentation, and terminal labeling with the GeneChip Whole Transcript Sense Target Labeling and Control Reagents (Affymetrix, Santa Clara, CA, USA). Then, it was processed for hybridization at 45°C for 17 h with Human Gene 1.0 ST Array (Affymetrix) containing 28,869 genes with approximately 26 probes per each gene that spread across the full length of the gene. The arrays were washed in the GeneChip Fluidic Station 450 (Affymetrix), and scanned by the GeneChip Scanner 3000 7G (Affymetrix). The data expressed as CEL files were normalized by the robust multiarray average (RMA) method with the Expression Console software version 1.1 (Affymetrix). By comparing the signal intensity levels between F3-WT and F3-Ngn1, the genes exhibiting either greater than twofold upregulation or smaller than 0.5-fold downregulation are considered as differentially expressed genes (DEG). To perform unsupervised clustering analysis of gene expression profiles, the CEL file-based data were imported to GeneSpring GX10 (Agilent).

Molecular Network Analysis

KeyMolnet is a comprehensive knowledgebase, originally established by the Institute of Medicinal Molecular Design (IMMD), Tokyo, Japan (Sato et al. 2005). It contains numerous contents of human genes, molecules and molecular relations, diseases, pathways, and drugs, all of which are manually collected, carefully curated, and regularly updated by expert biologists. The database is categorized into the core contents collected from selected review articles with the highest reliability or the secondary contents extracted from abstracts of PubMed database and Human Protein Reference database (HPRD). By importing the list of Entrez Gene ID and signal intensity data, KeyMolnet automatically provides corresponding molecules as a node on networks. Among various network-searching algorithms, the "N-points to N-points" search extracts the molecular network with the shortest route connecting the starting point molecules and the end point molecules. The generated network was compared side by side with 403 human canonical pathways of the KeyMolnet library. The algorithm counting the number of overlapping molecular relations between the extracted network and the canonical pathway makes it possible to identify the canonical pathway showing the most significant contribution to the extracted network. The significance in the similarity between both is scored following the formula, where $O =$ the number of overlapping molecular relations between the extracted network and the canonical pathway, $V =$ the number of molecular relations located in the extracted network, $C =$ the number of molecular relations located in the canonical pathway, $T =$ the number of total molecular relations composed of approximately 110,000 sets, and the $X =$ the sigma variable that defines coincidence.

$$\text{Score} = -\log_2(\text{Score (p)}) \quad \text{Score(p)} = \sum_{x=O}^{\text{Min}(C,V)} f(x)$$

$$f(x) = {}_C C_x \cdot {}_{T-C} C_{V-x} / {}_T C_V$$

Gene Annotation Analysis

Functional annotation of differentially expressed genes was searched by the web-accessible program named Database for Annotation, Visualization, and Integrated Discovery (DAVID) version 2008, National Institute of Allergy and Infectious Diseases (NIAID), NIH (david.abcc.ncifcrf.gov) (Huang da et al. 2009). It covers more than 40 annotation categories, including Gene ontology (GO) terms, protein–protein interactions, protein functional domains, disease associations, biological pathways, sequence general features, homologies, gene functional summaries, and tissue expressions. By importing the list of Entrez Gene ID, this program creates the functional annotation chart, an annotation-term-focused view that lists annotation terms and their associated genes under study. To avoid excessive counting of duplicated genes, the Fisher Exact statistics is calculated based on corresponding DAVID gene IDs by which all redundancies in original IDs are removed.

Real-Time RT-PCR Analysis

DNase-treated total cellular RNA was processed for cDNA synthesis using oligo(dT)$_{12-18}$ primers and SuperScript II reverse transcriptase (Invitrogen). Then, cDNA was amplified by PCR in LightCycler ST300 (Roche Diagnostics, Tokyo, Japan) using SYBR Green I and primer sets listed in Table 1. The expression levels of target genes were standardized against those of the glyceraldehyde-3-phosphate dehydrogenase (G3PDH) gene detected in parallel in identical cDNA samples. All the assays were performed in triplicate.

In some experiments, the ORF of Ngn1 was amplified by PCR using PfuTurbo DNA polymerase (Stratagene, La Jolla, CA, USA) and primer sets listed in Table 1. It was then cloned into the mammalian expression vector p3XFLAG-CMV7.1 (Sigma, St. Louis, MO, USA) to express a fusion protein with an N-terminal Flag tag. At 48 h after transfection of the vector in F3-WT cells by Lipofectamine 2000 reagent (Invitrogen), the cells were processed for real-time RT-PCR analysis of LGR5 and Western blot analysis of a Flag-fusion protein with anti-Flag M2 antibody (Sigma).

Table 1 Primers for RT-PCR and cloning utilized in the present study

Genes	GenBank accession no.	Sense primers	Antisense primers
NES	NM_006617	5′ctgctcaggagcagcactcttaac3′	5′cttagcctatgagatggagcaggc3′
LGR5	NM_003667	5′aacagtcctgtgactcaactcaag3′	5′ttagagacatgggacaaatgccac3′
GAS2	NM_005256	5′acaaacatgtcatggtccgtgtgg3′	5′aactggcagagaccaccaagtagt3′
HAS2	NM_005328	5′gccagctgccttagaggaaatatc3′	5′atggttttccttcctgatgtgccc3′
MMP9	NM_004994	5′tcttccagtaccgagagaaagcct3′	5′ctgcaggatgtcataggtcacgta3′
NEUROG1	NM_006161	5′ttcctcaccgacgaggaagactgt3′	5′tcaagttgtgcatgcggttgcgct3′
NEUROG1 for cloning	NM_006161	5′cggaattccccagcccgccttgagacctgc3′	5′cgggatcccgctagtggtaaggaatgaaac3′
G3PDH	NM_002046	5′ccatgttcgtcatgggtgtgaacca3′	5′gccagtagaggcagggatgatgttc3′

NES Nestin, *LGR5* leucine-rich repeat-containing G protein-coupled receptor 5, *GAS2* growth arrest-specific 2, *HAS2* hyaluronan synthase 2, *MMP9* matrix metallopeptidase 9, *NEUROG1* neurogenin 1, and *G3PDH* glyceraldehyde-3-phosphate dehydrogenase

Western Blot Analysis

To prepare total protein extract, the cells were homogenized in RIPA buffer containing a cocktail of protease inhibitors (Sigma). After separation on a 12% SDS-PAGE gel, the protein was transferred onto a nitrocellulose membrane, and the blot was incubated with rabbit polyclonal anti-LGR5 antibody (AP2745d) (ABGENT, Flanders Court, San Diego, CA, USA). Then, it was labeled with HRP-conjugated anti-rabbit IgG (Santa Cruz Biotechnology, Santa Cruz, CA, USA). The specific reaction was visualized by exposing of the blot to a chemiluminescence substrate (Pierce, Rockford, IL, USA). After the antibodies were stripped by incubating the membrane at 50°C for 30 min in stripping buffer, composed of 62.5 mM Tris–HCl, pH 6.7, 2% SDS, and 100 mM 2-mercaptoethanol, it was processed for relabeling with anti-Hsp60 antibody (N-20; Santa Cruz Biotechnology), an internal control for protein loading.

Results

Overexpression of Neurogenin 1 in F3-Ngn1 Cells

When incubated in the feeding medium, both F3-WT and F3-Ngn1 cells proliferated continuously with a doubling time ranging from 3 to 7 days. Although they were morphologically different, i.e. F3-WT exhibited a fusiform morphology, while F3-Ngn1 exhibited a cuboidal appearance (Fig. 1A, panels a and b), both of them expressed nestin but did not form a neurosphere when cultured in the feeding medium. The levels of expression of nestin mRNA were higher in F3-Ngn1 than F3-WT (Fig. 1B, panel a, lanes 1 and 2). Importantly, only F3-Ngn1 expressed Ngn1 mRNA (Fig. 1B, panel b, lanes 1 and 2).

We conducted genome-wide gene expression profiling of F3-WT and F3-Ngn1 by using two sets of Human Gene 1.0 ST Array for each, followed by two comparisons composed of F3-WT array-1 (WT-1) versus F3-Ngn1 array-1 (NGN-1) and F3-WT array-2 (WT-2) versus F3-Ngn1 array-2 (NGN-2). Unsupervised clustering analysis of these data clearly separated the cluster of F3-Ngn1 from that of F3-WT, based on gene expression profiles of 59 genes differentially expressed between both cell types (Fig. 2). The gene expression profile of WT-1 was similar to that of WT-2, while the gene expression profiles of NGN-1 and NGN-2 were almost identical, supporting the reproducibility among the results of repeated microarray analysis (Fig. 2). The analysis of individual probe data identified significant upregulation of Ngn1 ORF expression

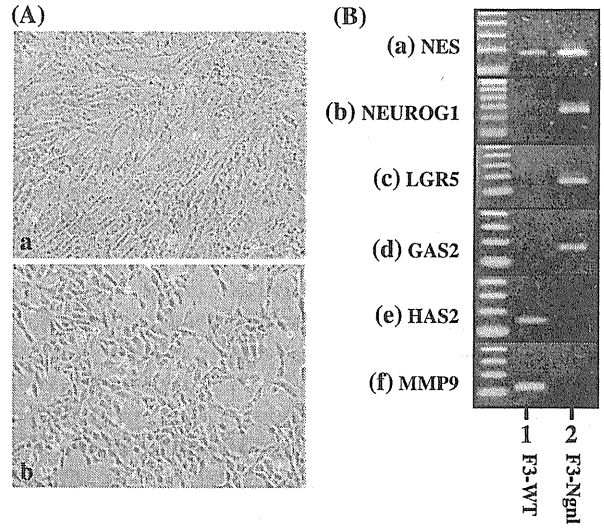

Fig. 1 Characterization of phenotypes of F3-WT and F3-Ngn1 cells. **A** Phase contrast photomicrograph. Both F3-WT cells (panel *a*) and F3-Ngn1 cells (panel *b*) were incubated in the feeding medium at a subconfluent density. **B** RT-PCR analysis. cDNA prepared from F3-WT cells (lane 1) and F3-Ngn1 cells (lane 2) was amplified by PCR for 30 cycles using primer sets listed in Table 1. The panels (*a–f*) represent (*a*) nestin (NES), (*b*) neurogenin 1 (NEUROG1), (*c*) leucine-rich repeat-containing G protein-coupled receptor 5 (LGR5), (*d*) growth arrest-specific 2 (GAS2), (*e*) hyaluronan synthase 2 (HAS2), and (*f*) matrix metallopeptidase 9 (MMP9)

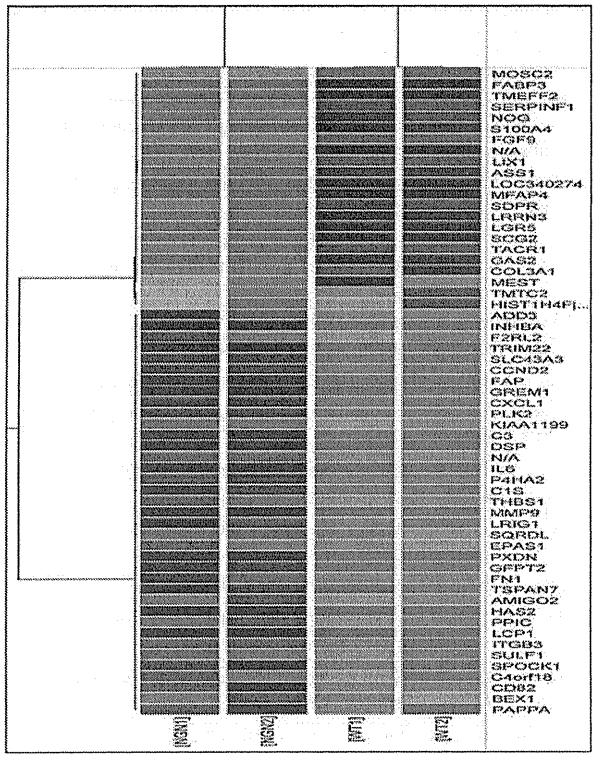

Fig. 2 Clustering analysis of gene expression profiles of F3-WT and F3-Ngn1 cells. Genome-wide gene expression profiling of F3-WT and F3-Ngn1 was performed by using two sets of Human Gene 1.0 ST Array for each, followed by two comparisons composed of WT array-1 (WT1) versus Ngn1 array-1 (NGN1) and WT array-2 (WT2) versus Ngn1 array-2 (NGN2). The microarray data are processed for unsupervised clustering analysis on GeneSpring GX10. A set of 59 differentially expressed genes between both cell types separated the cluster of F3-Ngn1 from that of F3-WT. The heat map represents upregulated genes (*orange*) and downregulated genes (*blue*)

in F3-Ngn1 cells (Supplementary Fig. 1). However, the Affymetrix GeneChip Command Console (AGCC) algorithm that calculates the cumulative gene expression levels excluded Ngn1 from the group of upregulated genes in F3-Ngn1 owing to low baseline expression of Ngn1 in the set of probes distributed outside its ORF on Human Gene 1.0 ST Array.

Microarray Analysis Identifies a Robust Induction of LGR5 in F3-Ngn1 Cells

Microarray analysis identified total 588 differentially expressed genes (DEG), composed of 250 upregulated genes and 338 downregulated genes in F3-Ngn1 versus F3-WT (see Supplementary Tables 1 and 2 for the complete lists). Top 20 upregulated genes are shown in Table 2. Notably, LGR5, a novel stem cell marker (Barker et al. 2007; Jaks et al. 2008; Sato et al. 2009), showed an 167-fold increase in F3-Ngn1 (Table 2; Fig. 3).

In view of cell type-specific markers for NSC, neurons, and glial cells, nestin (NES) exhibited a 3.1-fold increase in F3-Ngn1 (Supplementary Table 1; Fig. 3), consistent with RT-PCR results (Fig. 1B, panel a, lanes 1 and 2). However, the expression of other NSC-specific markers, such as musashi homolog 1 (MSI1) and ATP-binding cassette subfamily G member 2 (ABCG2), was not elevated in F3-Ngn1 (Fig. 3). Although neurofilament medium polypeptide (NEFM) showed a 2.1-fold increase, the expression of other neuron-specific markers, such as neurofilament heavy polypeptide (NEFH), enolase 2 (ENO2), and tubulin beta 3 (TUBB3), was not substantially upregulated in F3-Ngn1 (Fig. 3). The expression of astroglial (GFAP), oligodendroglial (MBP, MOG, and CNP), and microglial (CD68) markers remained unaltered (Fig. 3). Furthermore, NEUROD1, a putative Ngn-1 target gene,[5,10] was not upregulated in F3-Ngn1 (Fig. 3).

Top 20 downregulated genes are shown in Table 3. It is worthy to note that the great majority of top 20 downregulated genes are categorized as extracellular matrix-associated proteins.

RT-PCR and Western Blot Analysis Validated the Results of Microarray Analysis

Both the conventional RT-PCR and real-time RT-PCR analysis validated marked upregulation of LGR5 and GAS2, and remarkable downregulation of HAS2 and MMP9 in F3-Ngn1 (Fig. 1B, panels c–f, lanes 1 and 2; Fig. 4, panels a–d). Western blot analysis verified LGR5 protein expression exclusively in F3-Ngn1 (Fig. 4, panel e, lane 2).

To address the question whether LGR5 is a direct target for Ngn1, an expression vector of either Ngn1 or green fluorescent protein (GFP) was transfected in F3-WT cells (Fig. 5a, upper panel, lanes 1 and 2). At 48 h after transfection, the cells were processed for real-time RT-PCR analysis. Transient overexpression of Ngn1 did not induce LGR5 expression in F3-WT, suggesting that LGR5 is not a direct transcriptional target of Ngn1 (Fig. 5b).

An Involvement of the Complex Interaction of Networks Regulated by Multiple Transcription Factors in Development of F3-Ngn1 Cells

To clarify the molecular network of the genes differentially expressed between F3-WT and F3-Ngn1, we imported microarray data into KeyMolnet, a bioinformatics tool for analyzing molecular relations on a comprehensive knowledgebase. When Entrez Gene ID and expression levels of 588 DEG were imported, KeyMolnet recognized a set of 51 non-annotated genes to be removed. Then, it extracted 787

Table 2 Top 20 upregulated genes in F3 cells following stable expression of neurogenin 1

No.	Gene symbol	Fold change	Entrez gene ID	Gene name	Putative function
1	LGR5	166.623	8549	Leucine-rich repeat-containing G protein-coupled receptor 5	An orphan G protein-coupled receptor of the glycoprotein hormone receptor subfamily
2	GAS2	32.861	2620	Growth arrest-specific 2	A caspase-3 substrate that plays a role in regulating cell shape changes during apoptosis
3	FABP3	32.739	2170	Fatty acid-binding protein 3, muscle and heart (mammary-derived growth inhibitor)	A protein involved in intracellular metabolism of long-chain fatty acids and modulation of cell growth and proliferation
4	TMEFF2	28.233	23671	Transmembrane protein with EGF-like and two follistatin-like domains 2	A secreted protein with a EGF-like domain that promotes survival of hippocampal and mesencephalic neurons
5	LRRN3	24.284	54674	Leucine-rich repeat neuronal 3	An integral membrane protein of unknown function
6	SCG2	13.841	7857	Secretogranin II (chromogranin C)	A secretory protein involved in regulation of neurogenesis and angiogenesis
7	MFAP4	13.429	4239	Microfibrillar-associated protein 4	An extracellular matrix protein binding to both collagen and carbohydrate involved in cell adhesion
8	HIST1H4F	11.875	8361	H4 histone, family 2	A member of the histone H4 family that constitutes the nucleosome structure
9	TACR1	11.35	6869	Tachykinin receptor 1	A neurokinin receptor selective for substance P
10	COL3A1	10.828	1281	Collagen, type III, alpha 1	The pro-alpha 1 chains of type III collagen that constitutes a major component of the extracellular matrix
11	SDPR	9.975	8436	Serum deprivation response (phosphatidylserine-binding protein)	A calcium-independent phospholipid-binding protein that serves as a substrate of protein kinase C
12	TMTC2	9.744	160335	Transmembrane and tetratricopeptide repeat containing 2	An integral membrane protein of unknown function
13	FGF9	9.38	2254	Fibroblast growth factor 9 (glia-activating factor)	A member of the FGF family whose expression is dependent on Sonic hedgehog signaling
14	ASS1	8.813	445	Argininosuccinate synthetase 1	The enzyme that catalyzes the penultimate step of the arginine biosynthetic pathway
15	S100A4	8.555	6275	S100 calcium binding protein A4	A member of the S100 family of proteins involved in motility, invasion, and tubulin polymerization
16	LIX1	7.99	167410	Lix1 homolog (chicken)	A protein involved in RNA metabolism that has an essential function for motor neuron survival
17	FAM65B	7.974	9750	Family with sequence similarity 65, member B	a protein involved in myogenic cell differentiation
18	NOG	7.65	9241	Noggin	A secreted protein that plays a principal role in creating morphogenic gradients by antagonizing bone morphogenetic proteins
19	C1orf115	7.571	79762	Chromosome 1 open reading frame 115	An integral membrane protein of unknown function
20	CYSLTR2	7.23	57105	Cysteinyl leukotriene receptor 2	A G protein-coupled receptor for cysteinyl leukotrienes

Genome-wide gene expression profiling of F3-WT and F3-Ngn1 was performed by using two sets of Human Gene 1.0 ST Array for each, followed by two comparisons composed of WT array-1 (F3-WT-1) versus Ngn1 array-1 (F3-Ngn1-1) and WT array-2 (F3-WT-2) versus Ngn1 array-2 (F3-Ngn1-2). Top 20 upregulated genes in F3-Ngn1 cells are shown with fold change derived from the comparison between F3-WT-2 and F3-Ngn1-2

genes directly linked to the 537 genes. Subsequently, we performed the "N-points to N-points" search by starting from Ngn1 and ending with the set of 787 genes via the shortest route connecting starting and ending points. It generated a highly complex molecular network composed of 1,816 fundamental nodes and 7,238 molecular relations (Fig. 6). When the network was referred to the canonical pathways of the KeyMolnet library, the generated network has the most significant relationship with transcriptional regulation by nuclear factor kappa-B (NF-κB) with the score of 59.9 and score (p) = 9.467E−019. This was followed by transcriptional regulation by cyclic AMP-response element-binding protein (CREB) in the second rank with the score of 52.3 and score (p) = 1.771E−016, transcriptional regulation by vitamin D receptor (VDR) in the third rank with the score of 45.8 and score (p) = 1.582E−014, transcriptional

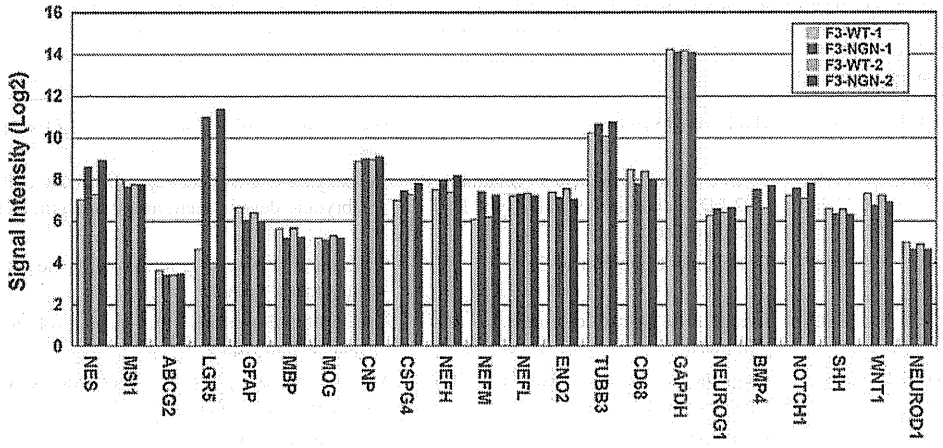

Fig. 3 Gene expression profiles of NSC, neuronal and glial markers. Genome-wide gene expression profiling of F3-WT and F3-Ngn1 was performed by using two sets of Human Gene 1.0 ST Array for each, followed by two comparisons composed of WT array-1 (F3-WT-1; the first column) versus Ngn1 array-1 (F3-Ngn1-1; the second column) and WT array-2 (F3-WT-2; the third column) versus Ngn1 array-2 (F3-Ngn1-2; the fourth column). Signal intensities of NSC, neuronal and glial marker genes are expressed as log 2 after normalization. *NES* nestin, *MSI1* musashi homolog 1, *ABCG2* ATP-binding cassette, subfamily G member 2, *LGR5* leucine-rich repeat-containing G protein-coupled receptor 5, *GFAP* glial fibrillary acidic protein, *MBP* myelin basic protein, *MOG* myelin oligodendrocyte glycoprotein, *CNP*, 2′3′-cyclic nucleotide 3′ phosphodiesterase, *CSPG4* chondroitin sulfate proteoglycan 4 (NG2), *NEFH* neurofilament heavy polypeptide, *NEFM* neurofilament medium polypeptide, *NEFL* neurofilament light polypeptide, *ENO2* enolase 2 (NSE), *TUBB3* tubulin beta 3, *GAPDH* glyceraldehyde-3-phosphate dehydrogenase (G3PDH), *NEUROG1* neurogenin 1, *BMP4* bone morphogenic protein 4, *NOTCH1* notch homolog 1, *SHH* sonic hedgehog homolog, *WNT1* wingless-type MMTV integration site family member 1, and *NEUROD1* neurogenic differentiation 1. A robust upregulation of LGR5 is evident in both F3-Ngn1-1 and F3-Ngn1-2

regulation by hypoxia-inducible factor (HIF) in the fourth rank with the score of 35.7 and score (p) = 1.781E−011, transcriptional regulation by glucocorticoid receptor (GR) in the fifth rank with the score of 31.0 and score (p) = 4.779E−010, and the complement activation pathway in the sixth rank with the score of 20.5 and score (p) = 6.589E−007. Thus, the molecular network of the genes differentially expressed between F3-WT and F3-Ngn1 involves the complex interaction of networks regulated by multiple transcription factors.

Gene Annotation Analysis Suggested Multifunctional Changes in F3-Ngn1 Cells

We studied functional annotation terms overrepresented in 588 DEG by using the web-accessible program named DAVID. By importing the list of Entrez Gene ID, DAVID identified top 20 enriched gene ontology (GO) terms in the list of 250 upregulated genes, most of which are related to development and morphogenesis (Table 4). In contrast, top 20 enriched GO terms in the list of 338 downregulated genes were chiefly composed of the molecules closely associated with extracellular matrix and adhesion (Table 4). Thus, gene annotation analysis suggested that stable expression of a single gene Ngn1 in F3 cells induces multifunctional changes that potentially affect the differentiation of human NSC.

Discussion

Recently, we established an immortalized human NSC clone named HB1.F3, which could serve as an unlimited source for cell replacement therapy of various neurological diseases (Kim 2004; Kim and de Vellis 2009). Ngn1 is a proneural bHLH transcription factor that promotes neuronal differentiation but inhibits glial differentiation of rodent NSC and NPC (Morrison 2001; Sun et al. 2001). In the present study, to investigate a role of Ngn1 in human NSC differentiation, we established a clone derived from F3 stably overexpressing Ngn1. Genome-wide gene expression profiling identified 250 upregulated genes and 338 downregulated genes in F3-Ngn1 versus F3-WT cells. Notably, the expression of LGR5, a recently identified marker for intestine and hair follicle stem cells (Barker et al. 2007; Jaks et al. 2008; Sato et al. 2009), was greatly elevated in F3-Ngn1 cells at both mRNA and protein levels. However, transient overexpression of Ngn1 did not induce upregulation of LGR5 in F3-WT cells, suggesting that LGR5 is not a direct transcriptional target of Ngn1. KeyMolnet, a bioinformatics tool for analyzing molecular relations on a comprehensive knowledgebase, indicated that the molecular network of differentially expressed genes involves the complex interaction of networks regulated by multiple transcription factors, such as NF-κB, CREB, VDR, HIF, and GR. Gene annotation analysis

Table 3 Top 20 downregulated genes in F3 cells following stable expression of neurogenin 1

No.	Gene symbol	Fold change	Entrez gene ID	Gene name	Putative function
1	HAS2	0.024	3037	Hyaluronan synthase 2	The enzyme involved in synthesis and transport of hyaluronic acid
2	MMP9	0.044	4318	Matrix metallopeptidase 9 (gelatinase B, 92 kDa gelatinase, 92 kDa type IV collagenase)	The enzyme that degrades type IV and V collagens involved in embryonic development and tissue remodeling
3	C3	0.05	718	Complement component 3	A protein that plays a central role in the activation of complement system
4	LCP1	0.05	3936	Lymphocyte cytosolic protein 1 (L-plastin)	An actin-binding protein that plays a role in cell adhesion-dependent signaling
5	PAPPA	0.068	5069	Pregnancy-associated plasma protein A, pappalysin 1	A secreted metalloproteinase which cleaves insulin-like growth factor binding proteins
6	DSP	0.072	1832	Desmoplakin	A component of functional desmosomes that anchors intermediate filaments to desmosomal plaques
7	SPOCK1	0.075	6695	Sparc/osteonectin, cwcv and kazal-like domains proteoglycan (testican) 1	A chondroitin sulfate/heparan sulfate proteoglycan expressed in the postsynaptic region of hippocampal pyramidal neurons
8	TRIM22	0.076	10346	Tripartite motif-containing 22	A member of the tripartite motif family induced by interferon and mediates interferon's antiviral effects
9	CCND2	0.087	894	Cyclin D2	A protein that forms a complex with CDK kinases involved in cell cycle G1/S transition
10	IL6	0.088	3569	Interleukin 6 (interferon, beta 2)	An immunoregulatory cytokine that functions in inflammation and the maturation of B cells
11	CD82	0.092	3732	CD82 molecule	A membrane glycoprotein activated by p53 involved in suppression of metastasis
12	SLC43A3	0.093	29015	Solute carrier family 43, member 3	An integral membrane protein of the SLC43A transporter family
13	GREM1	0.093	26585	Gremlin 1, cysteine knot superfamily, homolog (*Xenopus laevis*)	A member of bone morphogenic protein antagonist family expressed in the neural crest
14	INHBA	0.095	3624	Inhibin, beta A	A growth/differentiation factor for various cell types by acting as a homodimer (activin A) or a heterodimer (activin A-B)
15	ITGB3	0.095	3690	Integrin, beta 3 (platelet glycoprotein IIIa, antigen CD61)	A subunit of integrins involved in cell adhesion and cell-surface-mediated signaling
16	FAP	0.097	2191	Fibroblast activation protein, alpha	A homodimeric integral membrane gelatinase involved in epithelial–mesenchymal interactions during development
17	C1S	0.101	716	Complement component 1, s subcomponent	A major constituent of the human complement subcomponent C1 that associates with C1r and C1q to yield the first component of the serum complement system
18	PXDN	0.103	7837	Peroxidasin homolog (Drosophila)	An extracellular matrix-associated peroxidase involved in extracellular matrix consolidation
19	C4orf18	0.103	51313	Chromosome 4 open reading frame 18	A Golgi apparatus membrane of unknown function
20	CFH	0.104	3075	Complement factor H	Q serum glycoprotein that regulates the function of the alternative complement pathway

Genome-wide gene expression profiling of F3-WT and F3-Ngn1 was performed by using two sets of Human Gene 1.0 ST Array for each, followed by two comparisons composed of WT array-1 (F3-WT-1) versus Ngn1 array-1 (F3-Ngn1-1) and WT array-2 (F3-WT-2) versus Ngn1 array-2 (F3-Ngn1-2). Top 20 downregulated genes in F3-Ngn1 cells are shown with fold change derived from the comparison between F3-WT-2 and F3-Ngn1-2

suggested that GO terms of development and morphogenesis are enriched in upregulated genes, while those of extracellular matrix and adhesion are enriched in downregulated genes. These results suggest that stable expression of a single gene Ngn1 in F3 cells induces not simply neurogenic but multifunctional changes that potentially affect the differentiation of human NSC via a reorganization of complex gene regulatory networks.

LGR5, an orphan G protein-coupled receptor alternatively named GRP49 with structural similarity to the

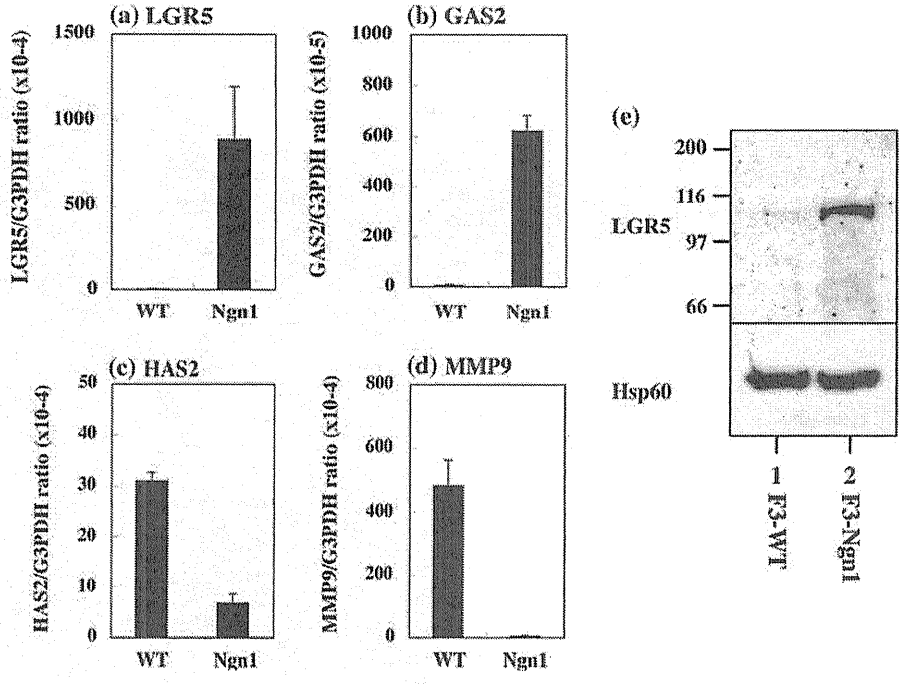

Fig. 4 Real-time RT-PCR and Western blot analysis. cDNA prepared from F3-WT and F3-Ngn1 cells was processed for real-time RT-PCR using primer sets listed in Table 1. Total protein extract was processed for western blot with anti-LGR5 antibody. The panels (**a–e**) represent real-time RT-PCR of **a** LGR5, **b** GAS2, **c** HAS2, and **d** MMP9, and western blot of (**e**, *upper panel*) LGR5 and (**e**, *lower panel*) Hsp60, an internal control for protein loading

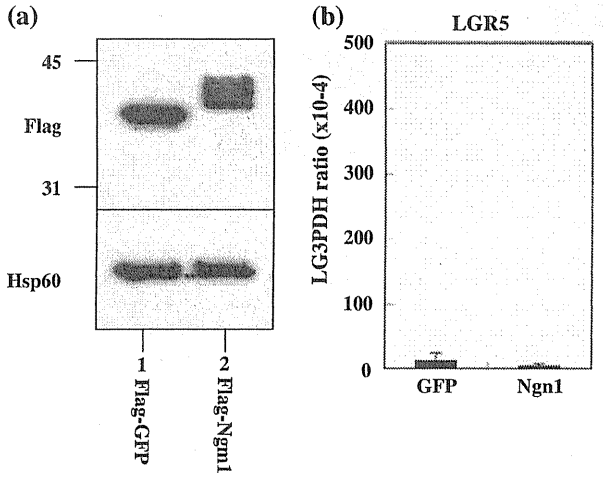

Fig. 5 Transient overexpression of Ngn1 did not induce upregulation of LGR5 in F3-WT cells. Expression vectors of Flag-tagged Ngn1 or GFP were transfected in F3-WT cells. At 48 h after transfection, the cells were processed for Western blot analysis of Flag and real-time RT-PCR analysis of LGR5. **a** Western blot analysis. The lanes (1, 2) represent *1* Flag-tagged GFP and *2* Flag-tagged Ngn1. The *upper panel* indicates Flag-tagged proteins, while the *lower panel* indicates Hsp60, an internal control for protein loading. **b** Real-time RT-PCR analysis. The *left bar* represents F3-WT cells with transient overexpression of Flag-tagged GFP, while the *right bar* represents those with transient overexpression of Flag-tagged Ngn1

glycoprotein hormone receptor family, is recently identified as a marker of adult intestinal stem cells and hair follicle stem cells by lineage-tracing studies (Barker et al. 2007; Jaks et al. 2008; Sato et al. 2009). LGR5 expression is also identified in the adult human spinal cord and brain at least at mRNA levels (Hsu et al. 1998). At present, the precise physiological function of LGR5 and downstream signaling pathways remain unknown owing to the lack of an identified natural ligand. LGR gene knockout mice showed neonatal lethality due to a breast-feeding defect caused by ankyloglossia, suggesting an involvement of LGR5 in craniofacial development (Morita et al. 2004). A more recent study showed that LGR5 deficiency induces premature differentiation of Paneth cells in the small intestine, accompanied by overactivation of the Wnt pathway, indicating that LGR5 acts as a negative regulator of Wnt (Garcia et al. 2009). A different study revealed that LGR5 is a marker for the sublineage of intestinal stem cells that are responsive to Wnt signals derived from stem cell niche (Ootani et al. 2009). In the populations of intestinal stem cells, LGR5 labels cycling cells, while doublecortin-like kinase-1 (DCLK1) marks quiescent cells (May et al. 2009). Interestingly, the expression of DCLK2, a putative paralog of DCLK1, is elevated with a 3.38-fold increase in F3-Ngn1 cells (Supplementary Table 1).

The interaction between Wnt proteins and Frizzled receptors on the cell surface transduces the signals to β-catenin by inactivating glycogen synthase kinase 3β (GSK3β), and stabilized β-catenin is translocated into the nucleus and forms a complex with T-cell factor (TCF) transcription factors to activate transcription of Wnt target genes. Importantly, LGR5 is identified as one of Wnt target genes (Yamamoto et al. 2003), suggesting a key role of LGR5 in establishment of a negative feedback loop in the

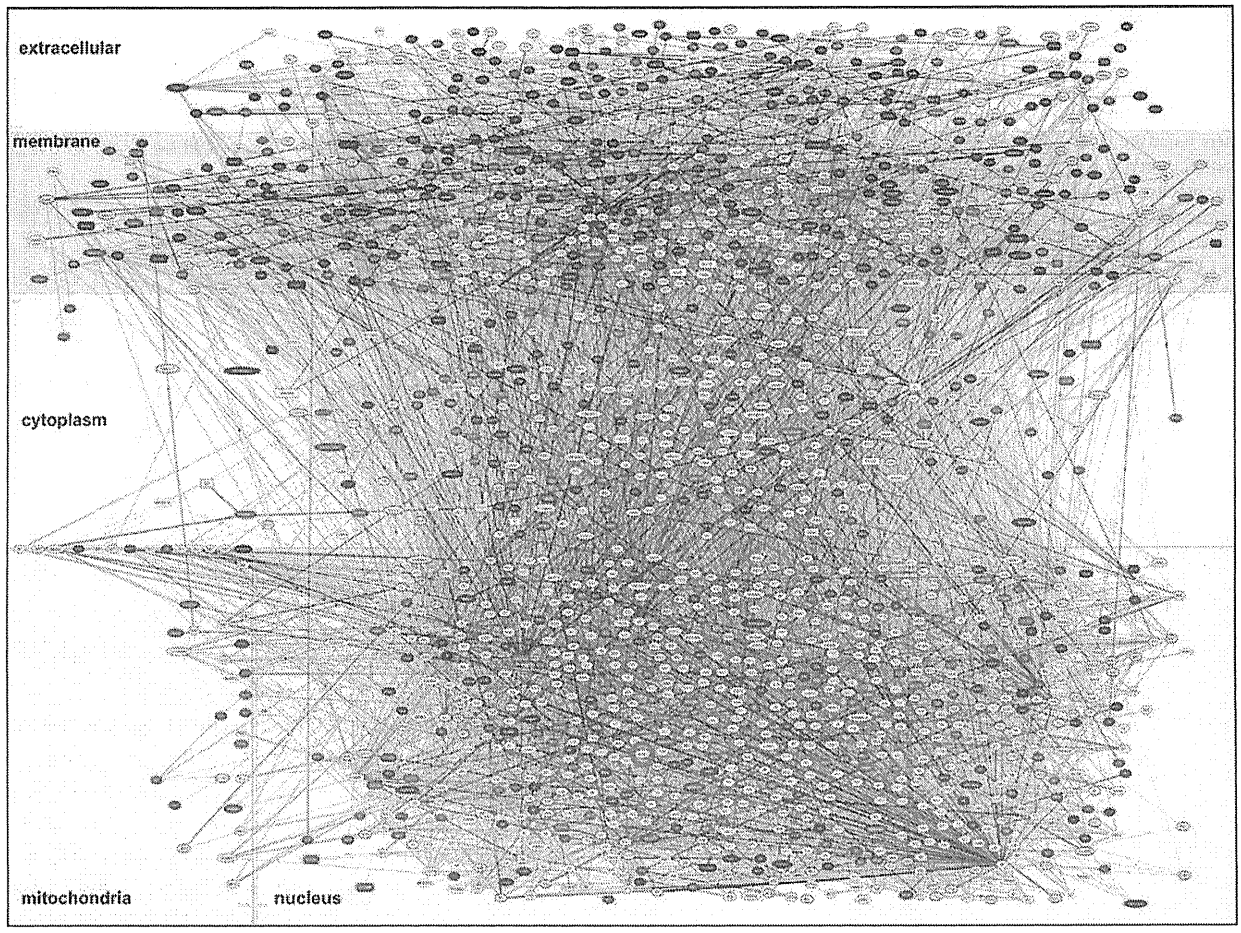

Fig. 6 Molecular network analysis of the genes regulated by stable expression of Ngn1 in F3 cells. The Entrez Gene ID and expression levels of 588 differentially expressed genes (DEG) between F3-WT and F3-Ngn1 cells were imported into KeyMolnet. It extracted 787 genes directly linked to the DEG. The "N-points to N-points" search was performed by starting from Ngn1 and ending with the set of 787 genes via the shortest route connecting starting and ending points. It generated a complex molecular network composed of 1,816 fundamental nodes and 7,238 molecular relations, arranged according to the subcellular location. *Red nodes* indicate upregulated genes, while *blue nodes* represent downregulated genes. *White nodes* exhibit additional molecules extracted automatically from KeyMolnet contents to establish molecular connections. The connections of *thick lines* represent the core contents, while *thin lines* indicate the secondary contents of KeyMolnet. The molecular relation is indicated by *dash line with arrow* (transcriptional activation), *solid line with arrow* (direct activation), or *solid line without arrow* (direct interaction or complex formation). Ngn1 is highlighted by a *purple circle*

Wnt pathway. In the present study, several Wnt target genes, such as FGF9 (Hendrix et al. 2006) and Dick homolog 1 (DKK1) (Niida et al. 2004), are coordinately upregulated, whereas MMP9 (Wu et al. 2007) is markedly downregulated in F3-Ngn1 (Tables 2 and 3; Supplementary Tables 1 and 2). FGF9 inhibits astrocyte differentiation of adult mouse NPC (Lum et al. 2009). One of us (SUK) recently found that DKK1 is a negative regulator of Wnt signaling in HB1.F3 cells (Ahn et al. 2008). MMP9 plays a central role in migration of adult NSC and NPC (Barkho et al. 2008). Interestingly, Ngn1 is also identified as a target of Wnt signaling, and it inhibits the self-renewal capacity of mouse cortical neural precursor cells (Hirabayashi et al. 2004). The expression of LGR5 is also controlled by the sonic hedgehog (SHH) signaling pathway (Tanese et al. 2008). SHH promotes Ngn1 expression in trigeminal neural crest cells (Ota and Ito 2003). Importantly, both Wnt and SHH signaling pathways play a central role in NSC development and differentiation (Prakash and Wurst 2007). Therefore, F3-Ngn1 cells might serve as a valuable tool for screening natural ligands of LGR5 that potentially affect the human NSC differentiation via Wnt and SHH signaling pathways, although it remains to be investigated whether a specialized subset of $LGR5^{+}$ NSC exists in vivo in the adult human central nervous system (CNS).

Table 4 Functional annotation terms of upregulated and downregulated genes in F3-Ngn1 cells

No.	Top 20 enriched GO terms in upregulated genes	*P* value	Top 20 enriched GO terms in downregulated genes	*P* value
1	GO:0048513 ~ organ development	4.71E−08	GO:0044421 ~ extracellular region part	1.66E−24
2	GO:0048731 ~ system development	5.15E−08	GO:0005576 ~ extracellular region	4.49E−22
3	GO:0048856 ~ anatomical structure development	1.32E−07	GO:0005578 ~ proteinaceous extracellular matrix	5.78E−15
4	GO:0007275 ~ multicellular organismal development	1.02E−06	GO:0031012 ~ extracellular matrix	9.50E−15
5	GO:0032502 ~ developmental process	1.73E−06	GO:0009605 ~ response to external stimulus	9.65E−14
6	GO:0009887 ~ organ morphogenesis	1.96E−06	GO:0005615 ~ extracellular space	1.42E−12
7	GO:0001501 ~ skeletal development	4.29E−05	GO:0009611 ~ response to wounding	2.42E−12
8	GO:0009653 ~ anatomical structure morphogenesis	5.80E−05	GO:0022610 ~ biological adhesion	3.08E−12
9	GO:0050793 ~ regulation of developmental process	1.46E−04	GO:0007155 ~ cell adhesion	3.08E−12
10	GO:0051216 ~ cartilage development	1.78E−04	GO:0048731 ~ system development	7.30E−10
11	GO:0007399 ~ nervous system development	1.97E−04	GO:0006954 ~ inflammatory response	1.24E−09
12	GO:0048754 ~ branching morphogenesis of a tube	2.23E−04	GO:0048856 ~ anatomical structure development	1.38E−09
13	GO:0001657 ~ ureteric bud development	2.37E−04	GO:0032502 ~ developmental process	1.87E−09
14	GO:0032501 ~ multicellular organismal process	2.47E−04	GO:0044420 ~ extracellular matrix part	2.45E−09
15	GO:0048598 ~ embryonic morphogenesis	2.48E−04	GO:0005581 ~ collagen	3.15E−09
16	GO:0030154 ~ cell differentiation	3.15E−04	GO:0007275 ~ multicellular organismal development	1.32E−08
17	GO:0048869 ~ cellular developmental process	3.15E−04	GO:0048513 ~ organ development	2.45E−08
18	GO:0000786 ~ nucleosome	3.33E−04	GO:0005509 ~ calcium ion binding	4.38E−08
19	GO:0043583 ~ ear development	3.42E−04	GO:0005125 ~ cytokine activity	6.33E−08
20	GO:0001763 ~ morphogenesis of a branching structure	3.42E−04	GO:0006950 ~ response to stress	1.21E−07

Functional annotation terms overrepresented in the list of 588 genes differentially expressed between F3-WT and F3-Ngn1 cells were searched on the web-accessible program named DAVID. Top 20 enriched gene ontology (GO) terms in 250 upregulated genes and top 20 enriched GO terms in 338 downregulated genes are shown with GO ID and *P* value

Acknowledgments This work was supported by a research grant to J-IS from the High-Tech Research Center Project, the Ministry of Education, Culture, Sports, Science and Technology (MEXT), Japan (S0801043), and from Research on Intractable Diseases, the Ministry of Health, Labour and Welfare of Japan. The microarray data are available from Gene Expression Omnibus (GEO) under the accession number GSE18296.

References

Ahn SM, Byun K, Kim D, Lee K, Yoo JS, Kim SU, Jho EH, Simpson RJ, Lee B (2008) Olig2-induced neural stem cell differentiation involves downregulation of Wnt signaling and induction of Dickkopf-1 expression. PLoS One 3:e3917

Barker N, van Es JH, Kuipers J, Kujala P, van den Born M, Cozijnsen M, Haegebarth A, Korving J, Begthel H, Peters PJ, Clevers H (2007) Identification of stem cells in small intestine and colon by marker gene Lgr5. Nature 449:1003–1007

Barkho BZ, Munoz AE, Li X, Li L, Cunningham LA, Zhao X (2008) Endogenous matrix metalloproteinase (MMP)-3 and MMP-9 promote the differentiation and migration of adult neural progenitor cells in response to chemokines. Stem Cells 26:3139–3149

Garcia MI, Ghiani M, Lefort A, Libert F, Strollo S, Vassart G (2009) LGR5 deficiency deregulates Wnt signaling and leads to precocious Paneth cell differentiation in the fetal intestine. Dev Biol 331:58–67

Hendrix ND, Wu R, Kuick R, Schwartz DR, Fearon ER, Cho KR (2006) Fibroblast growth factor 9 has oncogenic activity and is a downstream target of Wnt signaling in ovarian endometrioid adenocarcinomas. Cancer Res 66:1354–1362

Hirabayashi Y, Itoh Y, Tabata H, Nakajima K, Akiyama T, Masuyama N, Gotoh Y (2004) The Wnt/β-catenin pathway directs neuronal differentiation of cortical neural precursor cells. Development 131:2791–2801

Hsu SY, Liang SG, Hsueh AJ (1998) Characterization of two LGR genes homologous to gonadotropin and thyrotropin receptors with extracellular leucine-rich repeats and a G protein-coupled, seven-transmembrane region. Mol Endocrinol 12:1830–1845

Huang da W, Sherman BT, Lempicki RA (2009) Systematic and integrative analysis of large gene lists using DAVID bioinformatics resources. Nat Protoc 4:44–57

Jaks V, Barker N, Kasper M, van Es JH, Snippert HJ, Clevers H, Toftgård R (2008) Lgr5 marks cycling, yet long-lived, hair follicle stem cells. Nat Genet 40:1291–1299

Kim SU (2004) Human neural stem cells genetically modified for brain repair in neurological disorders. Neuropathology 24: 159–174

Kim SU, de Vellis J (2009) Stem cell-based cell therapy in neurological diseases: a review. J Neurosci Res 87:2183–2200

Kim S, Ghil SH, Kim SS, Myeong HH, Lee YD, Suh-Kim H (2002) Overexpression of neurogenin1 induces neurite outgrowth in F11 neuroblastoma cells. Exp Mol Med 34:469–475

Kim S, Yoon YS, Kim JW, Jung M, Kim SU, Lee YD, Suh-Kim H (2004) Neurogenin1 is sufficient to induce neuronal differentiation of embryonal carcinoma P19 cells in the absence of retinoic acid. Cell Mol Neurobiol 24:343–356

Kim SU, Park IH, Kim TH, Kim KS, Choi HB, Hong SH, Bang JH, Lee MA, Joo IS, Lee CS, Kim YS (2006) Brain transplantation of human neural stem cells transduced with tyrosine hydroxylase and GTP cyclohydrolase 1 provides functional improvement in animal models of Parkinson disease. Neuropathology 26: 129–140

Lum M, Turbic A, Mitrovic B, Turnley AM (2009) Fibroblast growth factor-9 inhibits astrocyte differentiation of adult mouse neural progenitor cells. J Neurosci Res 87:2201–2210

Ma Q, Fode C, Guillemot F, Anderson DJ (1999) Neurogenin1 and neurogenin2 control two distinct waves of neurogenesis in developing dorsal root ganglia. Genes Dev 13:1717–1728

May R, Sureban SM, Hoang N, Riehl TE, Lightfoot SA, Ramanujam R, Wyche JH, Anant S, Houchen CW (2009) DCAMKL-1 and LGR5 mark quiescent and cycling intestinal stem cells respectively. Stem Cells. doi:10.1002/stem.193

Morita H, Mazerbourg S, Bouley DM, Luo CW, Kawamura K, Kuwabara Y, Baribault H, Tian H, Hsueh AJ (2004) Neonatal lethality of LGR5 null mice is associated with ankyloglossia and gastrointestinal distension. Mol Cell Biol 24:9736–9743

Morrison SJ (2001) Neuronal differentiation: proneural genes inhibit gliogenesis. Curr Biol 11:R349–R351

Niida A, Hiroko T, Kasai M, Furukawa Y, Nakamura Y, Suzuki Y, Sugano S, Akiyama T (2004) DKK1, a negative regulator of Wnt signaling, is a target of the β-catenin/TCF pathway. Oncogene 23:8520–8526

Obayashi S, Tabunoki H, Kim SU, Satoh J (2009) Gene expression profiling of human neural progenitor cells following the serum-induced astrocyte differentiation. Cell Mol Neurobiol 29: 423–438

Ootani A, Li X, Sangiorgi E, Ho QT, Ueno H, Toda S, Sugihara H, Fujimoto K, Weissman IL, Capecchi MR, Kuo CJ (2009) Sustained in vitro intestinal epithelial culture within a Wnt-dependent stem cell niche. Nat Med 15:701–706

Ota M, Ito K (2003) Induction of neurogenin-1 expression by sonic hedgehog: its role in development of trigeminal sensory neurons. Dev Dyn 227:544–551

Prakash N, Wurst W (2007) A Wnt signal regulates stem cell fate and differentiation in vivo. Neurodegener Dis 4:333–338

Sato H, Ishida S, Toda K, Matsuda R, Hayashi Y, Shigetaka M, Fukuda M, Wakamatsu Y, Itai A (2005) New approaches to mechanism analysis for drug discovery using DNA microarray data combined with KeyMolnet. Curr Drug Discov Technol 2:89–98

Sato T, Vries RG, Snippert HJ, van de Wetering M, Barker N, Stange DE, van Es JH, Abo A, Kujala P, Peters PJ, Clevers H (2009) Single Lgr5 stem cells build crypt-villus structures in vitro without a mesenchymal niche. Nature 459:262–265

Sommer L, Ma Q, Anderson DJ (1996) Neurogenins, a novel family of atonal-related bHLH transcription factors, are putative mammalian neuronal determination genes that reveal progenitor cell heterogeneity in the developing CNS and PNS. Mol Cell Neurosci 8:221–241

Sun Y, Nadal-Vicens M, Misono S, Lin MZ, Zubiaga A, Hua X, Fan G, Greenberg ME (2001) Neurogenin promotes neurogenesis and inhibits glial differentiation by independent mechanisms. Cell 104:365–376

Tanese K, Fukuma M, Yamada T, Mori T, Yoshikawa T, Watanabe W, Ishiko A, Amagai M, Nishikawa T, Sakamoto M (2008) G-protein-coupled receptor GPR49 is up-regulated in basal cell carcinoma and promotes cell proliferation and tumor formation. Am J Pathol 173:835–843

Wu B, Crampton SP, Hughes CC (2007) Wnt signaling induces matrix metalloproteinase expression and regulates T cell transmigration. Immunity 26:227–239

Yamamoto Y, Sakamoto M, Fujii G, Tsuiji H, Kenetaka K, Asaka M, Hirohashi S (2003) Overexpression of orphan G-protein-coupled receptor, Gpr49, in human hepatocellular carcinomas with β-catenin mutations. Hepatology 37:528–533